AIMS Mathematics, 11(3): 7633–7658.
DOI: 10.3934/math.2026314
Received: 10 February 2026
Revised: 11 March 2026
Accepted: 17 March 2026
Published: 23 March 2026

https://www.aimspress.com/journal/Math

Research article

Fixed-time synchronization of memristive neural networks with time-varying delays via a new stability criterion

Junfeng Tong[1] **and Minghui Jiang**[2,*]

[1] College of Mathematics and Physics, China Three Gorges University, Yichang 443002, Hubei, China

[2] Three Gorges Mathematical Research Center, China Three Gorges University, Yichang 443002, Hubei, China

* **Correspondence:** Email: jiangminghui@ctgu.edu.cn.

Abstract: This paper investigates the fixed-time synchronization problem of memristive neural networks with time-varying delays by proposing a novel fixed-time stability theorem. Compared with existing results such as Lemmas 2.3 and 2.4, the proposed theorem provides a tighter upper bound estimate of the settling time, making the calculated convergence time closer to the actual evolution process of the system. Furthermore, the theorem removes the parameter constraints inherent in Lemma 2.5, thereby offering broader applicability. Based on the derived criteria, the influence of power function coefficients on the actual convergence rate is explored in detail. Finally, numerical simulations are provided to demonstrate the effectiveness and superiority of the theoretical results.

Keywords: differential equations; time-varying delay; memristor; neural networks; fixed-time synchronization
Mathematics Subject Classification: 34K20, 93D05, 93C10

1. Introduction

In recent years, artificial neural networks (ANNs) have established themselves as a cornerstone of modern computing, largely driven by their inherent strengths in handling parallel processing and complex pattern recognition [1–3]. A significant turning point occurred with the advent of memristive neural networks (MNNs), which have become a vibrant research frontier. This shift follows the 2008 physical realization of the memristor by Strukov's team [4], a breakthrough that confirmed Chua's 1971 prediction of the missing fourth passive circuit element [5]. By substituting conventional resistors in synapses with memristors, MNNs are distinguished by unique advantages, including non-volatility, high packing density, and nanoscale logical operations [6]. Consequently, the dynamic analysis of

MNNs has become a focal point for researchers in both engineering and applied mathematics [7–9].

As a fundamental collective behavior in nonlinear dynamical systems, synchronization plays a pivotal role in secure communications, image processing, and biological information processing [10–12]. Fruitful results have been achieved in this domain; for instance, Chen and Cao [13] investigated projective synchronization in drive-response systems, while Chen and Lu [14] explored cluster synchronization in complex networks. However, in practical hardware implementations, ideal delay-free systems are virtually non-existent. The presence of time delays is inescapable due to physical constraints, specifically the signal propagation duration among neurons and the restricted switching speeds of amplifiers. As noted by Cao and Wang [15], such time-varying delays can degrade system performance, potentially inducing oscillations, chaos, or even instability. Therefore, investigating the synchronization of MNNs subject to time-varying delays is of both profound theoretical value and urgent practical significance.

In control synthesis and synchronization analysis, the convergence rate serves as a critical metric for evaluating system performance.

- **Asymptotic Stability:** Early research primarily focused on asymptotic stability, where system states converge as time approaches infinity [16–18]. While theoretically sound, this paradigm often falls short of meeting the stringent requirements for rapid response and transient performance in modern engineering systems, such as missile guidance and high-frequency trading [19, 20].
- **Finite-time Stability:** To address the issue of infinite-time convergence, Bhat and Bernstein [20] introduced the concept of finite-time stability and provided rigorous Lyapunov criteria to ensure convergence within a finite duration. This concept was subsequently widely applied to neural network control [21, 22]. However, finite-time control suffers from a notable limitation: The settling time function is heavily dependent on the initial states of the system [23]. In other words, as the initial deviation increases, the time required for convergence grows. In practical applications where initial states are often unknown a priori or even unbounded, it becomes impossible to pre-estimate the exact convergence time.
- **Fixed-time Stability:** In an effort to mitigate the dependence on initial values, the concept of fixed-time stability was proposed in the seminal work of Polyakov [23]. This approach theoretically guarantees that the system stabilizes within a bounded interval, which remains invariant regardless of the initial conditions. This bounded convergence characteristic is crucial for applications where high-precision timing is a prerequisite [24, 25].

In recent years, researchers such as Chen et al. [25] have successfully applied fixed-time control theory to the synchronization of MNNs. Building upon the fixed-time stability framework, researchers have extended these results to more complex network models. For instance, Cao and Li [26] investigated the fixed-time synchronization problem for a class of recurrent neural networks with both memristive behaviors and communication delays, providing a specialized control scheme to ensure the synchronization error nullifies within a predictable time frame. This work is particularly relevant as it accounts for the non-linear switching characteristics inherent in memristive synapses. Despite these significant achievements, there remains room for improvement regarding the estimation accuracy of the settling time. The majority of existing literature [23] tends to employ standard scaling lemmas that estimate the settling time by simply algebraically superimposing the convergence times of two separate

phases [27–29]. This approach neglects the intrinsic coupling between system parameters, resulting in an upper bound for the settling time that is often overly conservative.

Driven by the limitations of current theoretical frameworks, we investigate the fixed-time synchronization of time-varying delayed MNNs. Unlike standard approaches, this work employs an optimized analytical strategy to derive a high-precision convergence time estimate, significantly mitigating the estimation errors inherent in existing literature.

Although substantial progress has been achieved in the fixed-time synchronization of neural networks, the conservatism associated with current settling time estimations remains a critical issue. Most existing literature relies on standard lemmas that estimate the settling time by simply summing the convergence times of two separate phases (e.g., the phase where the Lyapunov function $V(t) > 1$ and the phase where $0 < V(t) \leq 1$). This algebraic superposition ignores the coupling effects between system parameters, often leading to conservative estimates of the settling time upper bound. Furthermore, some existing criteria impose strict constraints on the exponential parameters (e.g., requiring the sum of exponents to equal 2), which limits the flexibility of the controller design. Therefore, developing a more refined estimation technique to obtain a tighter upper bound for the settling time is an open and challenging problem.

To bridge the gaps identified in current literature, we focus on the fixed-time synchronization control of MNNs with time-varying delays. The specific innovations and main contributions of this article are highlighted as follows:

(a) A novel fixed-time stability theorem is proposed to provide a more precise estimation of the settling time. Unlike traditional lemmas, the proposed theorem employs a partitioned integration strategy based on the magnitude relationship between the control gains (i.e., distinguishing between cases where $\lambda_1 < \lambda_2$ and $\lambda_1 > \lambda_2$).
(b) The conservatism of the settling time estimate is significantly reduced. Theoretical analysis and numerical comparisons demonstrate that the new upper bound is tighter than those derived from standard inequalities commonly used in previous studies.
(c) In the Example section, the influence of the values of λ_1 and λ_2 on the convergence rate of the system is discussed in depth.

In this paper, $\|\cdot\|_2$ denotes the Euclidean norm of a vector in $\mathbb{R}^n$, and $|\cdot|$ represents the absolute value of a scalar. The notation $\|e(t)\|_2 = \sqrt{\sum_{i=1}^{n} e_i^2(t)}$ is consistently used throughout the stability analysis and numerical simulations.

2. Preliminaries

This chapter considers the following memristive neural network (MNN) model with time-varying delays:

$$\dot{x}_i(t) = -b_i x_i(t) + \sum_{j=1}^{n} a_{ij}(x_i(t)) f_j(x_j(t)) + \sum_{j=1}^{n} c_{ij}(x_i(t)) g_j(x_j(t - \tau(t))) + I_i, \tag{2.1}$$

where $i \in \mathbb{N}_m$ and $j \in \mathbb{N}_n$. The scalar $x_i(t) \in \mathbb{R}$ represents the state of the ith neuron, $x(t) = (x_1(t), \ldots, x_n(t))^T \in \mathbb{R}^n$ is the state vector of the memristive neural network, and $b_i > 0$ denotes the self-inhibition coefficient. a_{ij} and c_{ij} represent the memristive connection weights; $f_j(\cdot)$ and $g_j(\cdot)$ are

the activation functions without and with time delays, respectively. $\tau(t)$ denotes the time-varying delay satisfying $0 \leq \tau(t) \leq \tau$, and I_i is the external input or bias. In the following, we introduce several basic definitions that will be used throughout this paper.

Definition 2.1. *Let A and B be two sets. A map $F : A \to B$ is called a set-valued map if for every $a \in A$, there corresponds a nonempty set $F(a) \subseteq B$, where $F(a)$ denotes the value or image of a under the map F.*

Definition 2.2. *A nonempty set-valued map $F : A \to B$ is said to be upper semicontinuous (USC) at $a_0 \in A$ if for any open set N containing $F(a_0)$, there exists a neighborhood M of a_0 such that $F(M) \subseteq N$. If $F(a)$ is closed (compact, convex) for all $a \in A$, then the map F is said to have closed (compact, convex) images.*

Definition 2.3. *[30] Consider the differential system $\dot{x}(t) = f(t, x)$ with the initial value $x_0 = x(0)$, where $f(t, x)$ is discontinuous. A function $x(t)$ is called a Filippov solution on a non-degenerate interval $[t_1, t_2]$ if $x(t)$ is absolutely continuous on $[t_1, t_2]$ and satisfies*

$$\dot{x}(t) \in K[f](t, x),$$

for almost all $t \in [t_1, t_2]$. Here, the set-valued map $K[f](t, x)$ is defined as

$$K[f](t, x) = \bigcap_{\delta>0} \bigcap_{\mu(N)=0} \overline{co}\left[f(B(x, \delta) \setminus N, t)\right],$$

where $\overline{co}[\cdot]$ denotes the closed convex hull, $B(x, \delta) = \{v : \|v - x\| \leq \delta\}$ represents the closed ball centered at x with radius $\delta > 0$, and $\mu(N)$ is the Lebesgue measure of the set N.

Based on the properties of the memristor, we have

$$a_{ij}(x_i(t)) = \begin{cases} a_{ij}^-, & |x_i(t)| \leq \Theta_i, \\ a_{ij}^+, & |x_i(t)| > \Theta_i, \end{cases}$$

$$c_{ij}(x_i(t)) = \begin{cases} c_{ij}^-, & |x_i(t)| \leq \Theta_i, \\ c_{ij}^+, & |x_i(t)| > \Theta_i, \end{cases}$$

where $\Theta_i > 0$ is the positive switching threshold constant, and $a_{ij}^-, a_{ij}^+, c_{ij}^-, c_{ij}^+$ are constants. The initial condition of system (2.1) is $x_i(t) = \varphi_i(s) \in C([-\tau, 0], \mathbb{R})$.

The memristive connection weights, $a_{ij}(\cdot)$ and $c_{ij}(\cdot)$, in the model considered here, are discontinuous functions. Consequently, conventional solution theories for differential equations are inapplicable since they require continuity. This necessitates the adoption of solutions in the sense of Filippov, a framework that rigorously handles the discontinuities inherent in the system's right-hand side.

Let $\check{a}_{ij} = \max\{a_{ij}^-, a_{ij}^+\}$, $\hat{a}_{ij} = \min\{a_{ij}^-, a_{ij}^+\}$, $\bar{a}_{ij} = \max\{|a_{ij}^-|, |a_{ij}^+|\}$, $\check{c}_{ij} = \max\{c_{ij}^-, c_{ij}^+\}$, $\hat{c}_{ij} = \min\{c_{ij}^-, c_{ij}^+\}$, and $\bar{c}_{ij} = \max\{|c_{ij}^-|, |c_{ij}^+|\}$. Then, based on the set-valued map, we have

$$K[a_{ij}(x_i(t))] = \begin{cases} a_{ij}^-, & |x_i(t)| < \Theta_i, \\ \text{co}\{\check{a}_{ij}, \hat{a}_{ij}\}, & |x_i(t)| = \Theta_i, \\ a_{ij}^+, & |x_i(t)| > \Theta_i, \end{cases}$$

$$K[c_{ij}(x_i(t))] = \begin{cases} c_{ij}^-, & |x_i(t)| < \Theta_i, \\ \text{co}\{\check{c}_{ij}, \hat{c}_{ij}\}, & |x_i(t)| = \Theta_i, \\ c_{ij}^+, & |x_i(t)| > \Theta_i, \end{cases}$$

where $K(E)$ denotes the closed convex hull of set E, and $\text{co}\{a, b\}$ represents the closed convex hull generated by a and b. When $f_j(\cdot)$ and $g_j(\cdot)$ are continuous functions, by virtue of the theories of differential inclusions and set-valued maps [31], system (2.1) can be rewritten in the form of the following differential inclusion:

$$\dot{x}_i(t) \in -b_i x_i(t) + \sum_{j=1}^{n} K[a_{ij}(x_i(t))] f_j(x_j(t)) + \sum_{j=1}^{n} K[c_{ij}(x_i(t))] g_j(x_j(t-\tau(t))) + I_i.$$

Suppose that $x_i(t)$ is a solution of system (2.1). According to the measurable selection theorem, which plays a pivotal role in handling the derivative of the Lyapunov function in the subsequent stability analysis, there exist bounded measurable selection functions $\hat{a}_{ij}(x_i(t)) \in K[a_{ij}(x_i(t))]$ and $\hat{c}_{ij}(x_i(t)) \in K[c_{ij}(x_i(t))]$ such that

$$\dot{x}_i(t) = -b_i x_i(t) + \sum_{j=1}^{n} \hat{a}_{ij}(x_i(t)) f_j(x_j(t)) + \sum_{j=1}^{n} \hat{c}_{ij}(x_i(t)) g_j(x_j(t-\tau(t))) + I_i. \tag{2.2}$$

Corresponding to the drive system (2.1), the response system is described as follows:

$$\dot{y}_i(t) = -b_i y_i(t) + \sum_{j=1}^{n} a_{ij}(y_i(t)) f_j(y_j(t)) + \sum_{j=1}^{n} c_{ij}(y_i(t)) g_j(y_j(t-\tau(t))) + I_i + u_i(t). \tag{2.3}$$

Similar to (2.2), there exist bounded measurable selection functions $\tilde{a}_{ij}(y_i(t)) \in K[a_{ij}(y_i(t))]$ and $\tilde{c}_{ij}(y_i(t)) \in K[c_{ij}(y_i(t))]$ such that

$$\dot{y}_i(t) = -b_i y_i(t) + \sum_{j=1}^{n} \tilde{a}_{ij}(y_i(t)) f_j(y_j(t)) + \sum_{j=1}^{n} \tilde{c}_{ij}(y_i(t)) g_j(y_j(t-\tau(t))) + I_i + u_i(t), \tag{2.4}$$

where $u_i(t)$ is the controller to be designed. The initial condition of system (2.4) is $y_i(t) = \phi_i(s) \in C([-\tau, 0], \mathbb{R})$. Define the synchronization error as $e_i(t) = y_i(t) - x_i(t)$. Then, from systems (2.2) and (2.4), the error system is obtained as

$$\dot{e}_i(t) = -b_i e_i(t) + \sum_{j=1}^{n} F_{ij}(t) + \sum_{j=1}^{n} G_{ij}(t), \tag{2.5}$$

where

$$\begin{aligned} F_{ij}(t) &= \tilde{a}_{ij}(y_i(t)) f_j(y_j(t)) - \hat{a}_{ij}(x_i(t)) f_j(x_j(t)), \\ G_{ij}(t) &= \tilde{c}_{ij}(y_i(t)) g_j(y_j(t-\tau(t))) - \hat{c}_{ij}(x_i(t)) g_j(x_j(t-\tau(t))). \end{aligned}$$

In the following, several necessary assumptions for this chapter are presented.

(A1) The activation functions $f_j(\cdot)$ and $g_j(\cdot)$ satisfy the Lipschitz condition. For any $j \in \mathbb{N}$, there exist non-negative constants M_j and N_j such that for any $x, y \in \mathbb{R}$,

$$|f_j(y) - f_j(x)| \leq M_j|y - x|, \quad |g_j(y) - g_j(x)| \leq N_j|y - x|.$$

(A2) The activation functions $f_j(\cdot)$ and $g_j(\cdot)$ are bounded. For any $j \in \mathbb{N}$, there exist non-negative constants F_j and G_j such that for any $x \in \mathbb{R}$,

$$|f_j(\cdot)| \leq F_j, \quad |g_j(\cdot)| \leq G_j.$$

Remark 2.1. *In this work, the Filippov solution is adopted to handle the discontinuities in $a_{ij}(\cdot)$ and $c_{ij}(\cdot)$ arising from the memristors' threshold-dependent switching. Assumptions (A1) and (A2) provide the necessary mathematical bounds (Lipschitz and boundedness) to facilitate the error system analysis. These foundational settings ensure that the drive-response systems (2.1) and (2.3) can achieve fixed-time synchronization under the proposed control laws.*

Lemma 2.1. *If **(A1)** and **(A2)** hold, then for any $x, y \in \mathbb{R}^n$, we have*

$$\begin{aligned}
&\left|K[a_{ij}(y)]f_j(y) - K[a_{ij}(x)]f_j(x)\right| \\
&= \left|K[a_{ij}(y)]f_j(y) + K[a_{ij}(y)]f_j(x) - K[a_{ij}(y)]f_j(x) - K[a_{ij}(x)]f_j(x)\right| \\
&\leq \left|K[a_{ij}(y)]f_j(y) - K[a_{ij}(y)]f_j(x)\right| + \left|K[a_{ij}(y)]f_j(x) - K[a_{ij}(x)]f_j(x)\right| \\
&\leq \bar{a}_{ij}M_j|y - x| + 2\bar{a}_{ij}F_j,
\end{aligned}$$

and, similarly,

$$\begin{aligned}
&\left|K[c_{ij}(y)]g_j(y) - K[c_{ij}(x)]g_j(x)\right| \\
&= \left|K[c_{ij}(y)]g_j(y) + K[c_{ij}(y)]g_j(x) - K[c_{ij}(y)]g_j(x) - K[c_{ij}(x)]g_j(x)\right| \\
&\leq \left|K[c_{ij}(y)]g_j(y) - K[c_{ij}(y)]g_j(x)\right| + \left|K[c_{ij}(y)]g_j(x) - K[c_{ij}(x)]g_j(x)\right| \\
&\leq \bar{c}_{ij}N_j|y - x| + 2\bar{c}_{ij}G_j.
\end{aligned}$$

Lemma 2.2. *[32] Let $x_1, x_2, \ldots, x_n \geq 0$, $0 < a \leq 1$, and $b > 1$. Then,*

$$\sum_{i=1}^{n} x_i^a \geq \left(\sum_{i=1}^{n} x_i\right)^a, \quad \sum_{i=1}^{n} x_i^b \geq n^{1-b}\left(\sum_{i=1}^{n} x_i\right)^b.$$

Definition 2.4. *[20] For the error $e_i(t)$ of the neural network -response system, if there exists a constant $T(e_0) > 0$ such that*

$$\lim_{t \to T(e_0)} \|e(t, x)\|_2 = 0,$$

and $\|e(t)\|_2 = 0$ for all $t \geq T(e_0)$, then the error system $e_i(t)$ of the neural network -response system is said to achieve finite-time synchronization, where $T(e_0)$ is called the settling time.

Definition 2.5. *[23] If the neural network satisfies the following two conditions,*

(1) The system and the response system achieve finite-time synchronization;

(2) For any initial value, there exists a constant $T > 0$ such that $T(e_0) \leq T$.

Then, the system and the response system are said to achieve fixed-time synchronization, where $T(e_0)$ is called the settling time.

Lemma 2.3. *[23] Assume that the system state equation is $\dot{x} = f(x)$, and there exists a continuous radially unbounded function $V(x) : \mathbb{R}^n \to \mathbb{R}_+ \cup \{0\}$ satisfying the following differential inequalities:*

(1) $V(e(t)) = 0 \iff e(t) = 0$,
(2) $\dot{V}(e(t)) \leq -\alpha V^p(e(t)) - \beta V^q(e(t))$,

where $\alpha, \beta > 0$ and $0 < p < 1 < q$. Then, system (2.5) is fixed-time stable, and $V(e(t)) = 0$ for all $t \geq T(e_0)$. The upper bound of the synchronization time $T(e_0)$ is given by

$$T(e_0) \leq T^1_{\max} = \frac{1}{\alpha(1-p)} + \frac{1}{\beta(q-1)}, \quad \forall e_0 \in \mathbb{R}^n.$$

Lemma 2.4. *[25] Assume that there exists a continuous radially unbounded function $V(x) : \mathbb{R}^n \to \mathbb{R}_+ \cup \{0\}$ satisfying the following differential inequalities:*

(1) $V(e(t)) = 0 \iff e(t) = 0$,
(2) $\dot{V}(e(t)) \leq -\alpha V^p(e(t)) - \beta V^q(e(t))$,

where $\alpha, \beta > 0$ and $0 < p < 1 < q$. Then, system (2.5) is fixed-time stable, and $V(e(t)) = 0$ for all $t \geq T(e_0)$. The upper bound of the synchronization time $T(e_0)$ is given by

$$T(e_0) \leq T^2_{\max} = \frac{1}{\alpha(1-p)} \left(\frac{\alpha}{\beta}\right)^{\frac{1-p}{q-p}} + \frac{1}{\beta(q-1)} \left(\frac{\alpha}{\beta}\right)^{\frac{1-q}{q-p}}, \quad \forall e_0 \in \mathbb{R}^n.$$

Lemma 2.5. *[33] Assume that there exists a continuous radially unbounded function $V(x) : \mathbb{R}^n \to \mathbb{R}_+ \cup \{0\}$ satisfying the following differential inequalities:*

(1) $V(e(t)) = 0 \iff e(t) = 0$,
(2) $\dot{V}(e(t)) \leq -\alpha V^p(e(t)) - \beta V^q(e(t))$,

where $\alpha, \beta > 0$, $p = 1 - \frac{1}{2\kappa}$, and $q = 1 + \frac{1}{2\kappa}$ with $\kappa > 0$. Then, system (2.5) is fixed-time stable, and $V(e(t)) = 0$ for all $t \geq T(e_0)$. The upper bound of synchronization time $T(e_0)$ is given by

$$T(e_0) \leq T^3_{\max} = \frac{\pi\kappa}{\sqrt{\alpha\beta}}, \quad \forall e_0 \in \mathbb{R}^n.$$

3. Main results

In this section, a novel fixed-time stability theorem is derived by employing variable substitution, definite integration techniques, and minimization analysis. Consequently, a more refined formula for estimating the upper bound of the settling time is presented.

3.1. New fixed-time stability criterion

Theorem 3.1. *Assume that there exists a continuous radially unbounded function $V(x) : \mathbb{R}^n \to \mathbb{R}_+ \cup \{0\}$ satisfying the following differential inequalities:*

(1) $V(e(t)) = 0 \iff e(t) = 0$,
(2) $\dot{V}(e(t)) \le -\alpha V^p(e(t)) - \beta V^q(e(t))$,

where $\alpha, \beta > 0$ and $0 < p < 1 < q$. Then, system (2.5) is fixed-time stable, and $V(e(t)) = 0$ for all $t \ge T(e_0)$. The least upper bound of the synchronization time $T(e_0)$ is given by:
i. *When $\alpha < \beta$,*

$$T(e_0) \le T^4_{\max} = \frac{1}{\alpha(1-p)}\left(\frac{\alpha}{\beta}\right)^{\frac{1-p}{q-p}} + \frac{1}{(\alpha+\beta)(q-1)}\left[\left(\frac{\alpha}{\beta}\right)^{\frac{1-q}{q-p}} - 1\right] + \frac{1}{\beta(q-1)};$$

ii. *When $\alpha > \beta$,*

$$T(e_0) \le T^5_{\max} = \frac{1}{\alpha(1-p)} + \frac{1}{(\alpha+\beta)(1-p)}\left[\left(\frac{\alpha}{\beta}\right)^{\frac{1-p}{q-p}} - 1\right] + \frac{1}{\beta(q-1)}\left(\frac{\alpha}{\beta}\right)^{\frac{1-q}{q-p}};$$

iii. *When $\alpha = \beta$, the least upper bound of $T(e_0)$ degenerates to $T^1_{\max}$ in Lemma 2.3.*

Proof. Let $W(s) = V^{1-p}(s)$. Then, taking the derivative yields $\dot{V}(s) = \frac{1}{1-p}\dot{W}(s)V^p(s)$. Substituting this into the inequality $\dot{V}(x(t)) \le -\alpha V^p(x(t)) - \beta V^q(x(t))$, we have

$$\frac{1}{1-p}\dot{W}(x(t))V^p(x(t)) \le -\alpha V^p(x(t)) - \beta V^q(x(t)).$$

Through simple algebraic manipulation, dividing both sides by $V^p(x(t))$ (for $V(x(t)) \neq 0$), we obtain

$$\dot{W}(x(t)) \le (1-p)\left[-\alpha - \beta V^{q-p}(x(t))\right] \le -\alpha(1-p).$$

That is,

$$\dot{W}(x(t)) \le -\alpha(1-p).$$

Consequently, there exists a positive constant $T(x(0)) = \frac{W(x(0))}{\alpha(1-p)}$ satisfying

$$\lim_{t \to T(x(0))} W(x(t)) = 0 \quad \text{and} \quad W(x(t)) = 0 \iff x(t) = 0.$$

Furthermore, the following equivalence relations hold:

$$W(x(t)) = 0 \iff V(x(t)) = 0 \iff x(t) = 0.$$

Thus, there exists a constant $T(x(0)) > 0$ such that for all $t \ge T(x(0))$, $\lim_{t \to T(x(0))} x(t) = 0$ and $x(t) \equiv 0$. According to Definition 2.4, the origin of the system is finite-time stable. It is straightforward to see that $T(x(0)) = \int_0^{T(x(0))} dt$.
Since $dt > 0$ and $\dot{V}(x(t)) = \frac{dV(x(t))}{dt} \le -\alpha V^p(x(t)) - \beta V^q(x(t)) < 0$, we have

$$dt \le \frac{dV(x(t))}{-\alpha V^p(x(t)) - \beta V^q(x(t))}.$$

To simplify the subsequent calculation, let $w = V(x(t))$. When $t = T(x(0))$, we have $\|x(t)\| = w = 0$. Thus, we obtain

$$T(x(0)) = \int_0^{T(x(0))} dt \leq \int_{V(x(0))}^0 \frac{dw}{-\alpha w^p - \beta w^q} = \int_0^{V(x(0))} \frac{dw}{\alpha w^p + \beta w^q}.$$

The subsequent calculation requires bounding the integrand. To ensure a more precise result, we first analyze the values of the dominant terms of the integrand, αw^p and βw^q. Based on the properties of power functions, it is known that there exists a constant $V^* = \left(\frac{\alpha}{\beta}\right)^{\frac{1}{q-p}} \in (0, V(x(0))]$ such that when $V(x(t)) \in (0, V^*]$, the inequality $\alpha w^p \geq \beta w^q$ holds. When $V(x(t)) \in (V^*, V(x(0))]$, we have $\alpha w^p \leq \beta w^q$. It can be observed that since the relationship between α and β is indeterminate, there are three cases for V^*: $V^* < 1$, $V^* > 1$, and $V^* = 1$. In the following, we discuss these three different cases respectively.
(1) When $\alpha < \beta$, we have $V^* < 1$. In this case, the interval of integration $(0, V(x(0))]$ is divided into three sub-intervals.
i. $0 < V(x(t)) \leq V^*$,

$$T^1(x(0)) \leq \int_0^{V^*} \frac{1}{\alpha w^p} dw = \frac{(V^*)^{1-p}}{\alpha(1-p)}.$$

ii. $V^* < V(x(t)) \leq 1$. In this interval, since $w \leq 1$ and $p < q$, we have $w^p \geq w^q$. Thus, $\alpha w^p + \beta w^q \geq \alpha w^q + \beta w^q$.

$$T^2(x(0)) \leq \int_{V^*}^1 \frac{1}{(\alpha+\beta) w^q} dw = \frac{(V^*)^{1-q} - 1}{(\alpha+\beta)(q-1)}.$$

iii. $1 < V(x(t)) \leq V(x(0))$,

$$T^3(x(0)) \leq \int_1^{V(x(0))} \frac{1}{\beta w^q} dw \leq \frac{1}{\beta(q-1)}.$$

In summary, when $\alpha < \beta$, $T(x(0)) = T^1(x(0)) + T^2(x(0)) + T^3(x(0))$. Therefore,

$$T(e_0) \leq T^4_{\max} = \frac{1}{\alpha(1-p)} \left(\frac{\alpha}{\beta}\right)^{\frac{1-p}{q-p}} + \frac{1}{(\alpha+\beta)(q-1)} \left[\left(\frac{\alpha}{\beta}\right)^{\frac{1-q}{q-p}} - 1\right] + \frac{1}{\beta(q-1)}.$$

(2) When $\alpha > \beta$, we have $V^* > 1$. In this case, the interval of integration $(0, V(x(0))]$ is divided into three sub-intervals.
i. $0 < V(x(t)) \leq 1$,

$$T^1(x(0)) \leq \int_0^1 \frac{1}{\alpha w^p} dw = \frac{1}{\alpha(1-p)}.$$

ii. $1 < V(x(t)) \leq V^*$. In this interval, since $w \geq 1$, we have $w^q \geq w^p$. Thus, $\alpha w^p + \beta w^q \geq \alpha w^p + \beta w^p$.

$$T^2(x(0)) \leq \int_1^{V^*} \frac{1}{(\alpha+\beta) w^p} dw = \frac{(V^*)^{1-p} - 1}{(\alpha+\beta)(1-p)}.$$

iii. $V^* < V(x(t)) \leq V(x(0))$,

$$T^3(x(0)) \leq \int_{V^*}^{V(x(0))} \frac{1}{\beta w^q} dw \leq \frac{(V^*)^{1-q}}{\beta(q-1)}.$$

In summary, when $\alpha > \beta$, $T(x(0)) = T^1(x(0)) + T^2(x(0)) + T^3(x(0))$. Therefore,

$$T(e_0) \le T^5_{\max} = \frac{1}{\alpha(1-p)} + \frac{1}{(\alpha+\beta)(1-p)}\left[\left(\frac{\alpha}{\beta}\right)^{\frac{1-p}{q-p}} - 1\right] + \frac{1}{\beta(q-1)}\left(\frac{\alpha}{\beta}\right)^{\frac{1-q}{q-p}}.$$

(3) When $\alpha = \beta$, we have $V^* = 1$. In this case, the interval of integration $(0, V(x(0))]$ is divided into two sub-intervals: $(0, 1]$ and $(1, V(x(0))]$.

$$T(x(0)) \le T^1_{\max} = \int_0^1 \frac{1}{\alpha w^p} dw + \int_1^{V(x(0))} \frac{1}{\beta w^q} dw \le \frac{1}{\alpha(1-p)} + \frac{1}{\beta(q-1)}.$$

This completes the proof of Theorem 3.1. □

Remark 3.1. *In the proof of Lemma 2.4, the relationship between the value of V^* and 1 was not considered. Instead, the integration interval $(0, V(x(0))]$ was directly divided, into two parts: $(0, V^*]$ and $(V^*, V(x(0))]$. In the proof of Theorem 3.1, it is straightforward to observe that when $\alpha < \beta$, Theorem 3.1 further refines the division of the interval $(V^*, V(x(0))]$ into two sub-intervals: $(V^*, 1]$ and $(1, V(x(0))]$. The core mechanism of this strategy is the introduction of the critical threshold $V^= (\alpha/\beta)^{1/(q-p)}$, which identifies the dominant term between αw^p and βw^q across different regions. By replacing the traditional algebraic superposition with this refined partitioned integration, the proposed method effectively captures the coupling effects between the gain coefficients α and β, leading to a tighter upper bound.*

In the interval $(V^*, 1]$, we have $w \le 1$, which implies $w^p \ge w^q$. Thus,

$$\alpha w^p + \beta w^q \ge \alpha w^q + \beta w^q \ge \beta w^q.$$

Consequently,

$$\frac{1}{\alpha w^p + \beta w^q} \le \frac{1}{\alpha w^q + \beta w^q} \le \frac{1}{\beta w^q}.$$

Therefore, comparing the corresponding terms in case (1) of the proof of Theorem 3.1, we have

$$T^2(x(0)) + T^3(x(0)) \le \frac{1}{(\alpha+\beta)(q-1)}\left[\left(\frac{\alpha}{\beta}\right)^{\frac{1-q}{q-p}} - 1\right] + \frac{1}{\beta(q-1)} \le \frac{1}{\beta(q-1)}\left(\frac{\alpha}{\beta}\right)^{\frac{1-q}{q-p}},$$

which implies $T^4_{\max} < T^2_{\max}$.

Similarly, when $\alpha > \beta$, in the interval $(1, V^*]$, we have $w \ge 1$, which implies $w^q \ge w^p$. Thus,

$$\alpha w^p + \beta w^q \ge \alpha w^p + \beta w^p \ge \alpha w^p.$$

Then, we have

$$\frac{1}{\alpha w^p + \beta w^q} \le \frac{1}{\alpha w^p + \beta w^p} \le \frac{1}{\alpha w^p}.$$

Therefore, for case (2) in the proof of Theorem 3.1, we have

$$T^1(x(0)) + T^2(x(0)) \le \frac{1}{(\alpha+\beta)(1-p)}\left[\left(\frac{\alpha}{\beta}\right)^{\frac{1-p}{q-p}} - 1\right] + \frac{1}{\beta(q-1)}\left(\frac{\alpha}{\beta}\right)^{\frac{1-q}{q-p}}$$

$$\leq \frac{1}{\alpha(1-p)} + \frac{1}{\beta(q-1)}\left(\frac{\alpha}{\beta}\right)^{\frac{1-q}{q-p}},$$

which implies $T^5_{\max} < T^2_{\max}$.

It is clearly true that $T^2_{\max}$ *is less than* $T^1_{\max}$ *[25]. From the above analysis, it can be concluded that when* $\alpha \neq \beta$*, the following inequalities hold:*

$$T^4_{\max} < T^2_{\max} < T^1_{\max}, \quad T^5_{\max} < T^2_{\max} < T^1_{\max}.$$

In particular, when $\alpha = \beta$*, we have*

$$T^5_{\max} = T^4_{\max} = T^2_{\max} = T^1_{\max}.$$

3.2. Fixed-time synchronization control

Next, in order to enable systems (2.2) and (2.4) to achieve synchronization within a fixed time, the following controller is designed:

$$u_i(t) = -\xi_{1i}e_i(t) - \text{sign}(e_i(t))\left(\xi_{2i} + \xi_{3i}|e_j(t-\tau(t))| + \xi_{4i}|e_i(t)|^{\theta_1} + \xi_{5i}|e_i(t)|^{\theta_2}\right), \tag{2.6}$$

where $\xi_{1i}, \xi_{2i}, \xi_{3i}$ are constants, $\xi_{4i} > 0, \xi_{5i} > 0$, $0 < \theta_1 < 1$, and $\theta_2 > 1$.

Theorem 3.2. *Under* ***(A1)*** *and* ***(A2)****, if* ξ_{1i}, ξ_{2i}*, and* ξ_{3i} *satisfy the following inequalities,*

$$\begin{cases} \xi_{1i} \geq -b_i + \dfrac{1}{2}\displaystyle\sum_{j=1}^{n}(\bar{a}_{ij} + \bar{a}_{ij}M_j^2), \\ \xi_{2i} \geq \displaystyle\sum_{j=1}^{n}(2\bar{a}_{ij}F_j + 2\bar{a}_{ij}G_j), \\ \xi_{3i} \geq \displaystyle\sum_{j=1}^{n}\bar{c}_{ij}N_j, \end{cases} \tag{2.7}$$

then, systems (2.2) and (2.4) can achieve synchronization within a fixed time under the action of the controller (2.6), and the settling time is estimated as

$$T(e_0) \leq T^6_{\max} = \frac{2}{\lambda_1(1-\theta_1)} + \frac{2}{\lambda_2(\theta_2-1)}, \tag{2.8}$$

where $\lambda_1 = 2^{\frac{\theta_1+1}{2}}\min\{\xi_{4i}\}$ *and* $\lambda_2 = 2^{\frac{\theta_2+1}{2}}n^{\frac{1-\theta_2}{2}}\min\{\xi_{5i}\}$.

Theorem 3.3. ***(A1)*** *and* ***(A2)*** *hold. Subject to the parameter constraints defined in (2.7), the controller (2.6) guarantees the fixed-time synchronization of the drive-response systems (2.2) and (2.4). Furthermore, the upper bound of the settling time is derived as*

$$T(e_0) \leq T^7_{\max} = \frac{2}{\lambda_1(1-\theta_1)}\left(\frac{\lambda_1}{\lambda_2}\right)^{\frac{1-\theta_1}{\theta_2-\theta_1}} + \frac{2}{\lambda_2(\theta_2-1)}\left(\frac{\lambda_1}{\lambda_2}\right)^{\frac{1-\theta_2}{\theta_2-\theta_1}}, \tag{2.9}$$

where $\lambda_1 = 2^{\frac{\theta_1+1}{2}}\min\{\xi_{4i}\}$ *and* $\lambda_2 = 2^{\frac{\theta_2+1}{2}}n^{\frac{1-\theta_2}{2}}\min\{\xi_{5i}\}$.

Theorem 3.4. *Suppose **(A1)** and **(A2)** hold. Subject to the constraints on parameters ξ_{1i}, ξ_{2i}, and ξ_{3i} defined in (2.7), the controller (2.6) ensures the fixed-time synchronization of the drive-response systems (2.2) and (2.4). Moreover, the settling time is bounded by*

$$T(e_0) \leq T^8_{\max} = \frac{\pi}{(1-\theta_1)\sqrt{\lambda_1\lambda_2}}, \tag{2.10}$$

where $\lambda_1 = 2^{\frac{\theta_1+1}{2}} \min\{\xi_{4i}\}$, $\lambda_2 = 2^{\frac{\theta_2+1}{2}} n^{\frac{1-\theta_2}{2}} \min\{\xi_{5i}\}$, and $\theta_1 + \theta_2 = 2$.

Theorem 3.5. *Suppose **(A1)** and **(A2)** hold. Subject to the parameter constraints on ξ_{1i}, ξ_{2i}, and ξ_{3i} defined in (2.7), the controller (2.6) guarantees the fixed-time synchronization of the drive-response systems (2.2) and (2.4). Furthermore, the upper bound of the settling time is derived as follows:*
i. *When $\lambda_1 < \lambda_2$,*

$$T(e_0) \leq T^9_{\max} = \frac{2}{\lambda_1(1-\theta_1)}\left(\frac{\lambda_1}{\lambda_2}\right)^{\frac{1-\theta_1}{\theta_2-\theta_1}} + \frac{2}{(\lambda_1+\lambda_2)(\theta_2-1)}\left[\left(\frac{\lambda_1}{\lambda_2}\right)^{\frac{1-\theta_2}{\theta_2-\theta_1}} - 1\right] + \frac{2}{\lambda_2(\theta_2-1)}.$$

ii. *When $\lambda_1 > \lambda_2$,*

$$T(e_0) \leq T^{10}_{\max} = \frac{2}{\lambda_1(1-\theta_1)} + \frac{2}{(\lambda_1+\lambda_2)(1-\theta_1)}\left[\left(\frac{\lambda_1}{\lambda_2}\right)^{\frac{1-\theta_1}{\theta_2-\theta_1}} - 1\right] + \frac{2}{\lambda_2(\theta_2-1)}\left(\frac{\lambda_1}{\lambda_2}\right)^{\frac{1-\theta_2}{\theta_2-\theta_1}}.$$

iii. *When $\lambda_1 = \lambda_2$, the least upper bound of $T(e_0)$ degenerates to $T^7_{\max}$ in Theorem 3.2, where $\lambda_1 = 2^{\frac{\theta_1+1}{2}} \min\{\xi_{4i}\}$,$\lambda_2 = 2^{\frac{\theta_2+1}{2}} n^{\frac{1-\theta_2}{2}} \min\{\xi_{5i}\}$.*

Proof. Consider the following Lyapunov function:

$$V(t) = \frac{1}{2}\sum_{i=1}^{n} \|e_i(t)\|_2^2 = \frac{1}{2}\sum_{i=1}^{n} (e_i(t))^2.$$

Differentiating $V(t)$ along the trajectories of system (2.5) yields

$$\begin{aligned}\frac{d}{dt}V(t) &= \sum_{i=1}^{n} e_i(t)\dot{e}_i(t) \\ &= \sum_{i=1}^{n} e_i(t)\Big[- b_i e_i(t) + \sum_{j=1}^{n} F_{ij}(t) + \sum_{j=1}^{n} G_{ij}(t) \\ &\quad - \xi_{1i}e_i(t) - \operatorname{sign}(e_i(t))\left(\xi_{2i} + \xi_{3i}|e_j(t-\tau(t))| + \xi_{4i}|e_i(t)|^{\theta_1} + \xi_{5i}|e_i(t)|^{\theta_2}\right)\Big].\end{aligned} \tag{2.11}$$

By Lemma 2.1, we have

$$\sum_{i=1}^{n} e_i(t)\sum_{j=1}^{n} F_{ij}(t) \leq \sum_{i=1}^{n} |e_i(t)|\left(\bar{a}_{ij}M_j|e_j(t)| + 2\bar{a}_{ij}F_j\right). \tag{2.12}$$

$$\sum_{i=1}^{n} e_i(t) \sum_{j=1}^{n} G_{ij}(t) \leq \sum_{i=1}^{n} |e_i(t)| \left(\bar{c}_{ij} N_j |e_j(t-\tau(t))| + 2\bar{c}_{ij} G_j \right). \tag{2.13}$$

Applying the Cauchy inequality, (2.12) can be transformed into

$$\begin{aligned} \sum_{i=1}^{n} |e_i(t)| \sum_{j=1}^{n} \left(\bar{a}_{ij} M_j |e_j(t)| + 2\bar{a}_{ij} F_j \right) \leq & \sum_{i=1}^{n} \sum_{j=1}^{n} \left(\frac{\bar{a}_{ij} |e_i(t)|^2}{2} + \frac{\bar{a}_{ij} M_j^2 |e_j(t)|^2}{2} \right) \\ & + \sum_{i=1}^{n} \sum_{j=1}^{n} 2\bar{a}_{ij} F_j |e_i(t)|. \end{aligned} \tag{2.14}$$

Substituting (2.13) and (2.14) into (2.11) yields

$$\begin{aligned} \frac{d}{dt} V(t) \leq & \sum_{i=1}^{n} \left\{ \left[-b_i + \frac{1}{2} \sum_{j=1}^{n} (\bar{a}_{ij} + \bar{a}_{ij} M_j^2) - \xi_{1i} \right] e_i^2(t) + \sum_{j=1}^{n} (2\bar{a}_{ij} F_j + 2\bar{a}_{ij} G_j - \xi_{2i}) |e_i(t)| \right. \\ & \left. + \sum_{j=1}^{n} (\bar{c}_{ij} N_j - \xi_{3i}) |e_j(t-\tau(t))| |e_i(t)| - \xi_{4i} |e_i(t)|^{\theta_1+1} - \xi_{5i} |e_i(t)|^{\theta_2+1} \right\} \\ \leq & - \sum_{i=1}^{n} \xi_{4i} |e_i(t)|^{\theta_1+1} - \sum_{i=1}^{n} \xi_{5i} |e_i(t)|^{\theta_2+1}. \end{aligned}$$

By Lemma 2.2, the above inequality can be transformed into

$$\frac{d}{dt} V(t) \leq - \sum_{i=1}^{n} \xi_{4i} |e_i(t)|^{\theta_1+1} - \sum_{i=1}^{n} \xi_{5i} |e_i(t)|^{\theta_2+1} \leq -\lambda_1 V^{\frac{\theta_1+1}{2}}(t) - \lambda_2 V^{\frac{\theta_2+1}{2}}(t). \tag{2.15}$$

Based on Lemma 2.3 and inequality (2.15), systems (2.4) and (2.6) achieve fixed-time synchronization, and the settling time is estimated by (2.8).

Analogously, by applying Lemma 2.4 to inequality (2.15), the fixed-time synchronization of the systems is guaranteed, with the settling time upper bound determined by (2.9).

Likewise, invoking Lemma 2.5 in conjunction with (2.15) validates the synchronization property, where the convergence time is calculated via (2.10).

Ultimately, utilizing the proposed Theorem 3.1 and inequality (2.15), the drive-response systems achieve fixed-time synchronization. The resulting settling time estimate corresponds to the formulation presented in Theorem 3.5.

The proof is thus completed. □

Remark 3.2. *When conducting stability analysis for nonlinear systems satisfying the differential inequality* $\dot{V}(t) \leq -\alpha V^p(t) - \beta V^q(t)$*, the estimation accuracy of the convergence time upper bound* $T_{\max}$ *is a critical metric for measuring control performance. Notably, this inequality is established as a global bound through rigorous parameter constraints rather than neglecting higher-order terms, which ensures the reliability of the* T_{max} *estimate. Compared with Lemmas 2.3–2.5 commonly used in existing literature, the proposed Theorem 3.1 possesses significant theoretical advantages:*

(i) ***Overcoming estimation conservatism:*** *Lemma 2.3 serves as a fundamental criterion, obtaining* $T^1_{\max}$ *by simply summing the time estimates of two convergence stages (*$V > 1$ *and* $0 < V \leq 1$*). Its result is often conservative as it fails to accurately reflect the coupling effect between gain coefficients* α *and* β*. Although Lemma 2.4 improves estimation accuracy using the gain ratio, Theorem 3.1 provides the currently tightest time bound estimation by performing a refined piecewise integration analysis based on the relationship between the magnitudes of* α *and* β *(i.e.,* $\alpha < \beta$ *vs.* $\alpha > \beta$*).*

(ii) ***Relaxing the exponential symmetry constraint:*** *Lemma 2.5 can only provide an analytical optimal solution under the strict symmetric condition where the exponents satisfy* $p + q = 2$*. In contrast, the proposed Theorem 3.1 only requires the general constraint* $0 < p < 1 < q$*. As brilliantly pointed out by the theoretical analysis, by relaxing the rigid exponential symmetry constraint (*$p + q = 2$*) required by Lemma 2.5, Theorem 3.1 offers enhanced design flexibility and broader universality. This significantly expands the applicability of the fixed-time control framework in complex asymmetric parameter designs.*

(iii) ***Theoretical consistency and completeness:*** *Theorem 3.1 demonstrates excellent degeneration characteristics. When the system gains satisfy* $\alpha = \beta$*, the estimated values* $T^4_{\max}$ *or* $T^5_{\max}$ *given by Theorem 3.1 simplify directly to the classical form of* $T^1_{\max}$ *in Lemma 2.3. This consistency verifies that Theorem 3.1 is an effective generalization and deepening of existing theories.*

In summary, Theorem 3.1 not only achieves mathematical compatibility with existing lemmas, but also realizes breakthroughs in parameter selection flexibility and time estimation accuracy. While the five-term controller structure (2.6) implies a higher degree of complexity compared to traditional single-term designs,potentially increasing hardware resource consumption and computational overhead in memristive circuit implementations,it provides the necessary mathematical degrees of freedom for the piecewise integration strategy. This strategy effectively captures the coupling between control gains to significantly reduce estimation conservatism, providing superior theoretical guidance and a flexible design trade-off for the high-precision synchronization control of subsequent multi-agent systems.

4. Example

In this section, numerical simulation experiments are conducted to verify the system synchronization under four different parameter cases: $\lambda_1 < \lambda_2$ with $\theta_1+\theta_2 \neq 2$, $\lambda_1 > \lambda_2$ with $\theta_1+\theta_2 \neq 2$, $\lambda_1 < \lambda_2$ with $\theta_1 + \theta_2 = 2$, and $\lambda_1 > \lambda_2$ with $\theta_1 + \theta_2 = 2$. Moreover, a comparative analysis is performed between the theoretical synchronization time estimates derived from the theorems and the actual synchronization times observed in the simulations.

Example 4.1. This example, together with Examples 4.2 and 4.3, discusses the synchronization of the system under the conditions $\lambda_1 < \lambda_2$ and $\theta_1 + \theta_2 \neq 2$. Consider the following driving memristive neural networks with time-varying delays:

$$\begin{cases} \dot{x}_1(t) = -b_1 x_1(t) + \bar{a}_{11}(x_1(t)) f_1(x_1(t)) + \bar{a}_{12}(x_1(t)) f_2(x_2(t)) \\ \qquad + \bar{c}_{11}(x_1(t)) g_1(x_1(t-\tau(t))) + \bar{c}_{12}(x_1(t)) g_2(x_2(t-\tau(t))) + I_1, \\ \dot{x}_2(t) = -b_2 x_2(t) + \bar{a}_{21}(x_2(t)) f_1(x_1(t)) + \bar{a}_{22}(x_2(t)) f_2(x_2(t)) \\ \qquad + \bar{c}_{21}(x_1(t)) g_1(x_1(t-\tau(t))) + \bar{c}_{22}(x_1(t)) g_2(x_2(t-\tau(t))) + I_2, \end{cases} \tag{2.16}$$

where $I_1 = I_2 = 0$, the switching threshold $\Theta_i = 1$, and the time-varying delay $\tau(t) = 0.2\sin(t)$. The activation functions are chosen as $f_j(\cdot) = g_j(\cdot) = \tanh(\cdot)$. It is straightforward to verify that $\tanh(\cdot)$ satisfies the conditions in **(A1)** and **(A2)**,

$$\begin{pmatrix} M_1 & M_2 \\ N_1 & N_2 \end{pmatrix} = \begin{pmatrix} 1 & 1 \\ 1 & 1 \end{pmatrix}, \quad \begin{pmatrix} F_1 & F_2 \\ G_1 & G_2 \end{pmatrix} = \begin{pmatrix} 1 & 1 \\ 1 & 1 \end{pmatrix}.$$

The self-feedback coefficients of the system are set as $(b_1, b_2)^T = (1.2, 0.8)^T$, and the memristive connection weights are defined as follows:

$$a_{11}(x_1(t)) = \begin{cases} 2.5, & |x_1(t)| \le 1, \\ -2, & |x_1(t)| > 1, \end{cases} \qquad a_{12}(x_1(t)) = \begin{cases} 0.8, & |x_1(t)| \le 1, \\ 0.3, & |x_1(t)| > 1, \end{cases}$$

$$a_{21}(x_2(t)) = \begin{cases} -1.5, & |x_2(t)| \le 1, \\ 2, & |x_2(t)| > 1, \end{cases} \qquad a_{22}(x_2(t)) = \begin{cases} 1.3, & |x_2(t)| \le 1, \\ 0.4, & |x_2(t)| > 1, \end{cases}$$

$$c_{11}(x_1(t)) = \begin{cases} 1.5, & |x_1(t)| \le 1, \\ 0.8, & |x_1(t)| > 1, \end{cases} \qquad c_{12}(x_1(t)) = \begin{cases} 0.6, & |x_1(t)| \le 1, \\ -2, & |x_1(t)| > 1, \end{cases}$$

$$c_{21}(x_2(t)) = \begin{cases} -1.5, & |x_2(t)| \le 1, \\ 3.6, & |x_2(t)| > 1, \end{cases} \qquad c_{22}(x_2(t)) = \begin{cases} 1.2, & |x_2(t)| \le 1, \\ -0.3, & |x_2(t)| > 1. \end{cases}$$

The corresponding response memristive neural networks are described as follows:

$$\begin{cases} \dot{y}_1(t) = -b_1 y_1(t) + \bar{a}_{11}(y_1(t)) f_1(y_1(t)) + \bar{a}_{12}(y_1(t)) f_2(y_2(t)) \\ \qquad + \bar{c}_{11}(y_1(t)) g_1(y_1(t-\tau(t))) + \bar{c}_{12}(y_1(t)) g_2(y_2(t-\tau(t))) + I_1 + u_1, \\ \dot{y}_2(t) = -b_2 y_2(t) + \bar{a}_{21}(y_2(t)) f_1(y_1(t)) + \bar{a}_{22}(y_2(t)) f_2(y_2(t)) \\ \qquad + \bar{c}_{21}(y_1(t)) g_1(y_1(t-\tau(t))) + \bar{c}_{22}(y_1(t)) g_2(y_2(t-\tau(t))) + I_2 + u_2. \end{cases} \tag{2.17}$$

According to the definition, we have:

$$\begin{pmatrix} \bar{a}_{11} & \bar{a}_{12} \\ \bar{a}_{21} & \bar{a}_{22} \end{pmatrix} = \begin{pmatrix} 2.5 & 0.8 \\ 2 & 1.3 \end{pmatrix}, \quad \begin{pmatrix} \bar{c}_{11} & \bar{c}_{12} \\ \bar{c}_{21} & \bar{c}_{22} \end{pmatrix} = \begin{pmatrix} 1.5 & 2 \\ 3.6 & 1.2 \end{pmatrix}.$$

The state trajectories of the system without the controller u_i are illustrated in Figure 1. Based on the calculation of the aforementioned parameters, the relevant parameters of the controller can be determined as follows:

$$\xi_{11} = 2.5 > -b_1 + \frac{1}{2}\sum_{j=1}^{2} \bar{a}_{1j}(1 + M_j^2) = 2.1, \qquad \xi_{12} = 3 > -b_2 + \frac{1}{2}\sum_{j=1}^{2} \bar{a}_{2j}(1 + M_j^2) = 2.5.$$

$$\xi_{21} = 13.5 > \sum_{j=1}^{n}(2\bar{a}_{1j}F_j + 2\bar{a}_{1j}G_j) = 13.2, \qquad \xi_{22} = 13.5 > \sum_{j=1}^{n}(2\bar{a}_{2j}F_j + 2\bar{a}_{2j}G_j) = 13.2.$$

$$\xi_{31} = 4 > \bar{c}_{11}N_1 + \bar{c}_{12}N_2 = 3.5, \qquad \xi_{32} = 5 > \bar{c}_{21}N_1 + \bar{c}_{22}N_2 = 4.8.$$

The initial values of the system and the response system are given as $x_i(0) = (4, -5)^T$ and $y_i(0) = (-6, 3)^T$. The parameters are selected as $\theta_1 = 0.6$, $\theta_2 = 1.6$, $(\xi_{41}, \xi_{42})^T = (4, 6)^T$, and $(\xi_{51}, \xi_{52})^T = (4.4, 7)^T$.

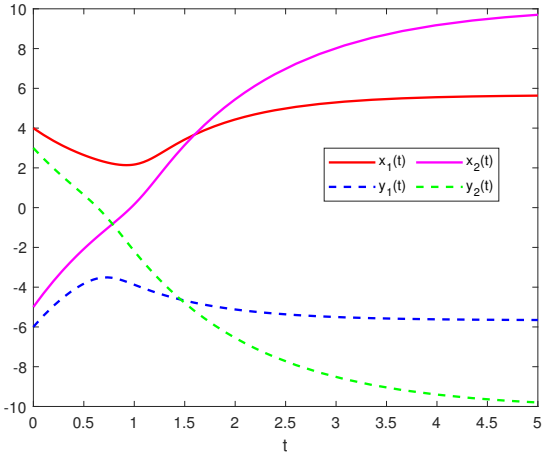

Figure 1. State trajectories of the system without controllers.

Based on the aforementioned parameter selection, calculations yield $\lambda_1 = 2^{0.8} \times 4 = 6.96$ and $\lambda_2 = 2 \times 4.4 = 8.80$. In this case, we have $\frac{\lambda_1}{\lambda_2} \approx 0.8 < 1$. With the selected parameters, under the controllers u_1 and u_2, the synchronization trajectories of the systems (2.16) and (2.17) are shown in Figure 2, and the synchronization error curves are shown in Figure 3. Meanwhile, the actual synchronization time of system under the current parameter selection is obtained as $T_{\text{sync}} = 0.1350$.

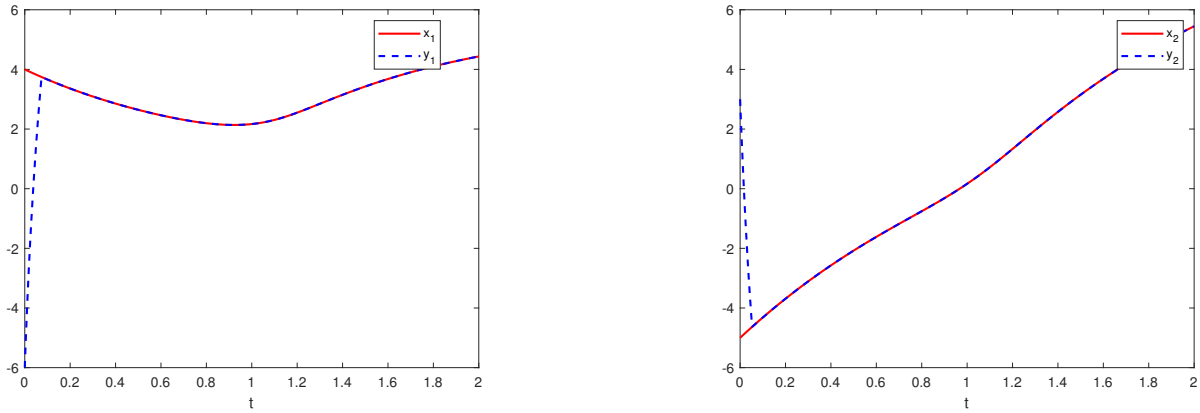

Figure 2. State trajectories of the system under controllers u_1 and u_2.

From Eq (2.8), it is known that $T^6_{\max} = 1.10$ in Theorem 3.2. From Eq (2.9), it is known that $T^7_{\max} = 1.09$ in Theorem 3.3. According to Theorem 3.5, $T^9_{\max} = 1.06$. Since $\theta_1 + \theta_2 = 2.4 \neq 2$ in this

example, Theorem 3.4 is not applicable.

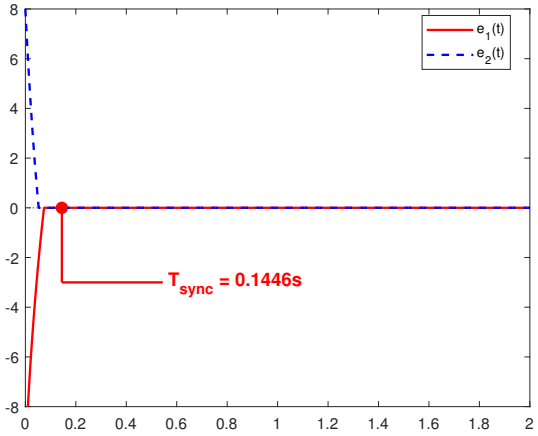

Figure 3. Applying the controller u_1 and u_2 system error curve.

Remark 4.1. *In practical engineering, the threshold Θ_i corresponds to the normalized critical voltage for resistance state switching in physical memristors, while the sinusoidal delay $\tau(t)$ is adopted to simulate the bounded and continuous fluctuations of transmission delays caused by limited amplifier switching speeds or network congestion in real hardware implementations.*

Example 4.2. Consider the model in Example 4.1 with all other conditions remaining unchanged. Set the parameters in the controller (2.6) as $(\xi_{41}, \xi_{42})^T = (4, 6)^T$, $(\xi_{51}, \xi_{52})^T = (8, 7)^T$, and $(\theta_1, \theta_2)^T = (0.6, 1.6)^T$. It is readily obtained that $\frac{\lambda_1}{\lambda_2} \approx 0.5 < 1$. In this case, under the controller (2.6), the synchronization error curves of systems (2.16) and (2.17) are shown in Figure 4. Meanwhile, the actual synchronization time of the system under the current parameter selection is obtained as $T_{\text{sync}} = 0.1270$. Through calculation, the theoretical synchronization times derived from Theorems 3.2, 3.3, and 3.5 are $T^6_{\max} = 0.96$, $T^7_{\max} = 0.90$, and $T^9_{\max} = 0.86$, respectively.

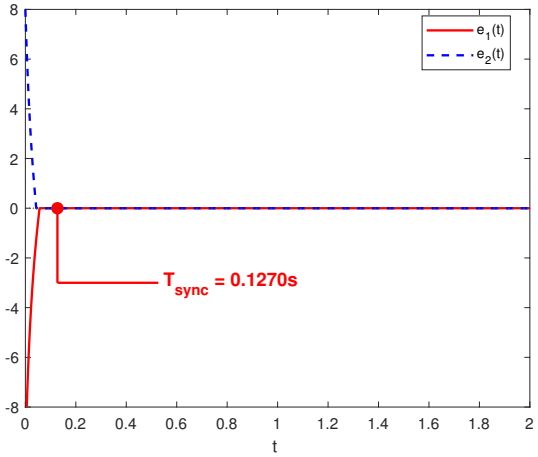

Figure 4. Example 4.2 systematic error curve.

Example 4.3. Consider the model in Example 4.1 with all other conditions remaining unchanged. Set the parameters in the controller (2.6) as $(\xi_{41}, \xi_{42})^T = (4, 6)^T$, $(\xi_{51}, \xi_{52})^T = (12, 10)^T$, and $(\theta_1, \theta_2)^T = (0.6, 1.6)^T$. It is readily obtained that $\frac{\lambda_1}{\lambda_2} \approx 0.35 < 1$.

In this case, under the controller (2.6), the synchronization error curves of system (2.16) and system (2.17) are shown in Figure 5. Meanwhile, the actual synchronization time of the system under the current parameter selection is obtained as $T_{\text{sync}} = 0.1223$. Through calculation, the theoretical synchronization times derived from Theorems 3.2, 3.3, and 3.5 are $T^6_{\max} = 0.88$, $T^7_{\max} = 0.78$, and $T^9_{\max} = 0.75$, respectively.

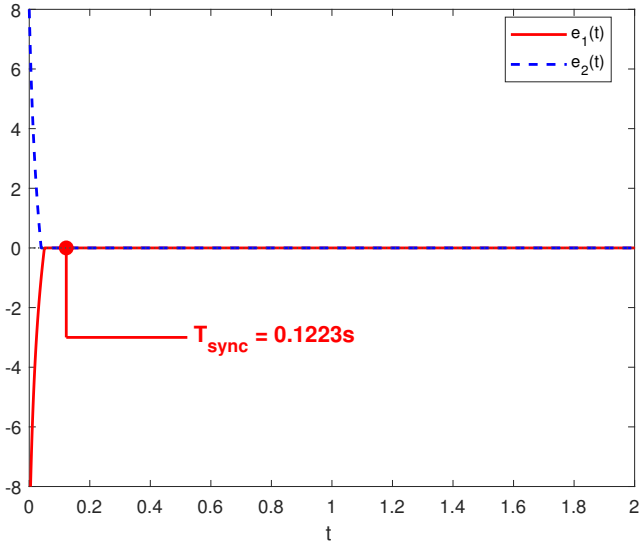

Figure 5. Example 4.3 systematic error curve.

Example 4.4. This example, together with Examples 4.5 and 4.6, discusses the synchronization of the system under the conditions $\lambda_1 > \lambda_2$ and $\theta_1 + \theta_2 \neq 2$.

Consider the model in Example 2.1 with all other conditions remaining unchanged. Set the parameters in the controller (2.6) as $(\xi_{41}, \xi_{42})^T = (10, 11)^T$, $(\xi_{51}, \xi_{52})^T = (3, 2)^T$, and $(\theta_1, \theta_2)^T = (0.6, 1.6)^T$. It is readily obtained that $\frac{\lambda_1}{\lambda_2} \approx 4.35 > 1$.

In this case, under the controller (2.6), the synchronization error curves of systems (2.16) and (2.17) are shown in Figure 6. Meanwhile, the actual synchronization time of the system under the current parameter selection is obtained as $T_{\text{sync}} = 0.1387$. Through calculation, the theoretical synchronization times derived from Theorems 3.2, 3.3, and 3.5 are $T^6_{\max} = 1.12$, $T^7_{\max} = 0.86$, and $T^{10}_{\max} = 0.82$, respectively.

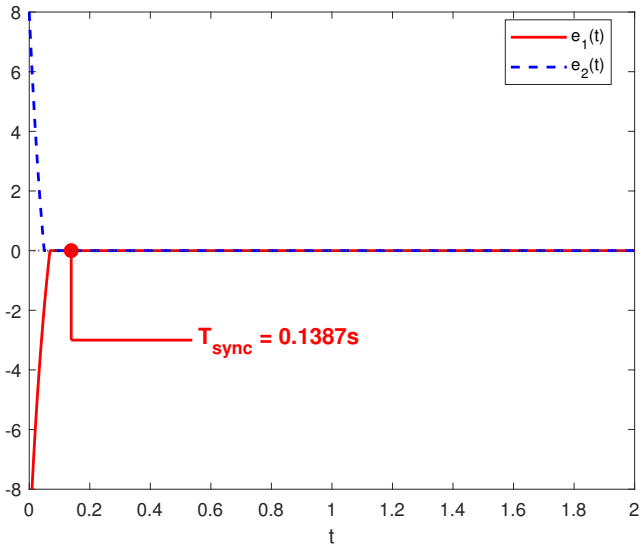

Figure 6. Example 4.4 systematic error curve.

Example 4.5. Consider the model in Example 4.1 with all other conditions remaining unchanged. Set the parameters in the controller (2.6) as $(\xi_{41}, \xi_{42})^T = (4.7, 6)^T$, $(\xi_{51}, \xi_{52})^T = (3, 2)^T$, and $(\theta_1, \theta_2)^T = (0.6, 1.6)^T$. It is readily obtained that $\frac{\lambda_1}{\lambda_2} \approx 2.05 > 1$.

In this case, under the controller (2.6), the synchronization error curves are shown in Figure 7. Meanwhile, the actual synchronization time of the system under the current parameter selection is obtained as $T_{\text{sync}} = 0.1446$. Through calculation, the theoretical synchronization times derived from Theorems 3.2, 3.3, and 3.5 are $T^6_{\max} = 1.44$, $T^7_{\max} = 1.36$, and $T^{10}_{\max} = 1.29$, respectively.

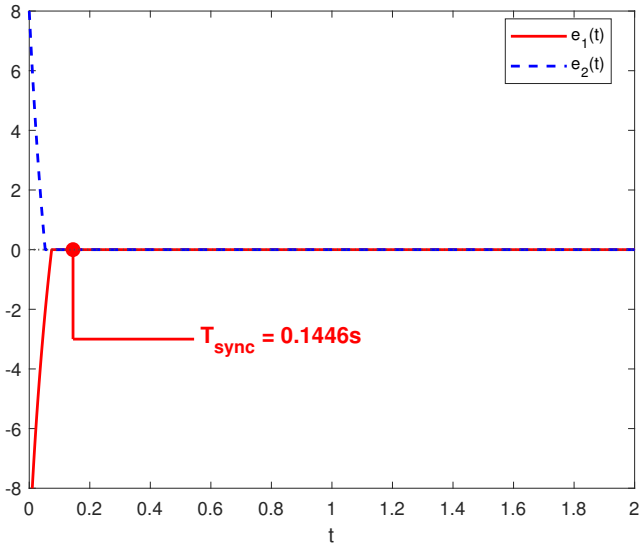

Figure 7. Example 4.5 systematic error curve.

Example 4.6. Consider the model in Example 4.1 with all other conditions remaining unchanged. Set the parameters in the controller (2.6) as $(\xi_{41}, \xi_{42})^T = (2.5, 3)^T$, $(\xi_{51}, \xi_{52})^T = (3, 2)^T$, and $(\theta_1, \theta_2)^T =$

$(0.6, 1.6)^T$. It is readily obtained that $\frac{\lambda_1}{\lambda_2} \approx 1.10 > 1$.

In this case, under the controller (2.6), the synchronization error curves are shown in Figure 8. Meanwhile, the actual synchronization time of the system under the current parameter selection is obtained as $T_{\text{sync}} = 0.1451$. Through calculation, the theoretical synchronization times derived from Theorems 3.2, 3.3, and 3.5 are $T^6_{\max} = 1.99$, $T^7_{\max} = 1.98$, and $T^{10}_{\max} = 1.96$, respectively.

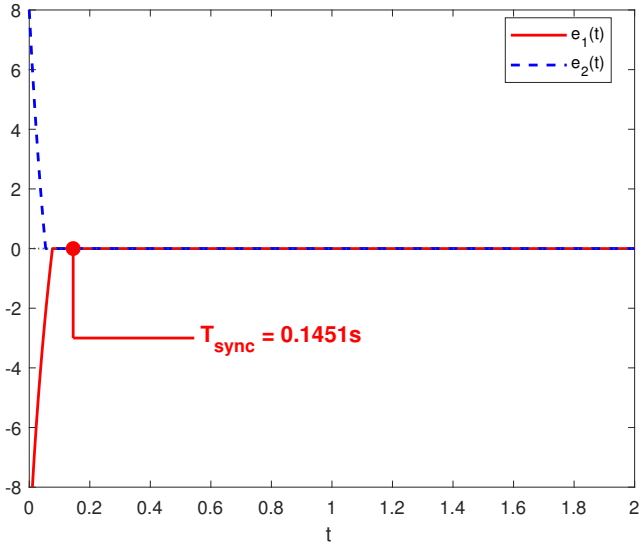

Figure 8. Example 4.6 systematic error curve.

Example 4.7. This example discusses the synchronization of the system under the conditions $\lambda_1 < \lambda_2, \theta_1 + \theta_2 = 2$ and $\lambda_1 > \lambda_2, \theta_1 + \theta_2 = 2$.

Consider the model in Example 4.1 with all other conditions remaining unchanged. Set the parameters in the controller (2.6) as $(\xi_{41}, \xi_{42})^T = (4, 6)^T$, $(\xi_{51}, \xi_{52})^T = (4.4, 7)^T$, and $(\theta_1, \theta_2)^T = (0.6, 1.4)^T$. It is readily obtained that $\frac{\lambda_1}{\lambda_2} \approx 0.8 < 1$.

In this case, the synchronization error curves are shown in Figure 3. The actual synchronization time under the current parameter selection is obtained as $T_{\text{sync}} = 0.1392$. The theoretical synchronization times calculated from Theorems 3.4 and 3.5 are $T^8_{\max} = 1.00$ and $T^9_{\max} = 1.25$, respectively.

Next, set the parameters as $(\xi_{41}, \xi_{42})^T = (4, 6)^T$, $(\xi_{51}, \xi_{52})^T = (12, 10)^T$, and $(\theta_1, \theta_2)^T = (0.6, 1.4)^T$. It is readily obtained that $\frac{\lambda_1}{\lambda_2} \approx 0.35 < 1$.

In this scenario, the synchronization error curves are shown in Figure 5. The actual synchronization time of the system under the current parameter selection is obtained as $T_{\text{sync}} = 0.1285$. The theoretical synchronization times calculated from Theorems 3.4 and 3.5 are $T^8_{\max} = 0.67$ and $T^9_{\max} = 0.80$, respectively.

Set the parameters as $(\xi_{41}, \xi_{42})^T = (4.7, 6)^T$, $(\xi_{51}, \xi_{52})^T = (3, 2)^T$, and $(\theta_1, \theta_2)^T = (0.6, 1.4)^T$. It is readily obtained that $\frac{\lambda_1}{\lambda_2} \approx 2.05 > 1$.

In this case, the synchronization error curves are shown in Figure 8. The actual synchronization time under the current parameter selection is obtained as $T_{\text{sync}} = 0.1479$. The theoretical synchronization times calculated from Theorems 3.4 and 3.5 are $T^8_{\max} = 1.37$ and $T^{10}_{\max} = 1.66$, respectively.

Set the parameters as $(\xi_{41}, \xi_{42})^T = (10, 11)^T$, $(\xi_{51}, \xi_{52})^T = (3, 2)^T$, and $(\theta_1, \theta_2)^T = (0.6, 1.4)^T$. It is

readily obtained that $\frac{\lambda_1}{\lambda_2} \approx 4.35 > 1$.

In this scenario, the synchronization error curves are shown in Figure 6. The actual synchronization time under the current parameter selection is obtained as $T_{\text{sync}} = 0.1415$. The theoretical synchronization times calculated from Theorems 3.4 and 3.5 are $T^8_{\max} = 0.94$ and $T^{10}_{\max} = 1.14$, respectively.

From the aforementioned numerical simulation experiments, it is observed that the inequalities $T^9_{\max} < T^7_{\max} < T^6_{\max}$ consistently hold when $\lambda_1 < \lambda_2$, and $T^{10}_{\max} < T^7_{\max} < T^6_{\max}$ consistently hold when $\lambda_1 > \lambda_2$. These simulation results effectively validate the effectiveness of Theorem 3.1. Furthermore, as illustrated in Figures 9 and 10, the theoretical synchronization time upper bound provided by Theorem 3.1 is closer to the actual synchronization time of the system compared to those derived from Lemmas 2.3 and 2.4.

The values of $T^8_{\max}$ in Lemma 2.5 and $T^9_{\max}$ and $T^{10}_{\max}$ in Theorem 3.1 under different conditions are listed in Table 1. Although $T^8_{\max}$ is smaller than $T^9_{\max}$ or $T^{10}_{\max}$ within the selected parameter range, its applicability is less extensive than that of Theorem 3.1 due to the constraint on the exponents $\theta_1+\theta_2 = 2$.

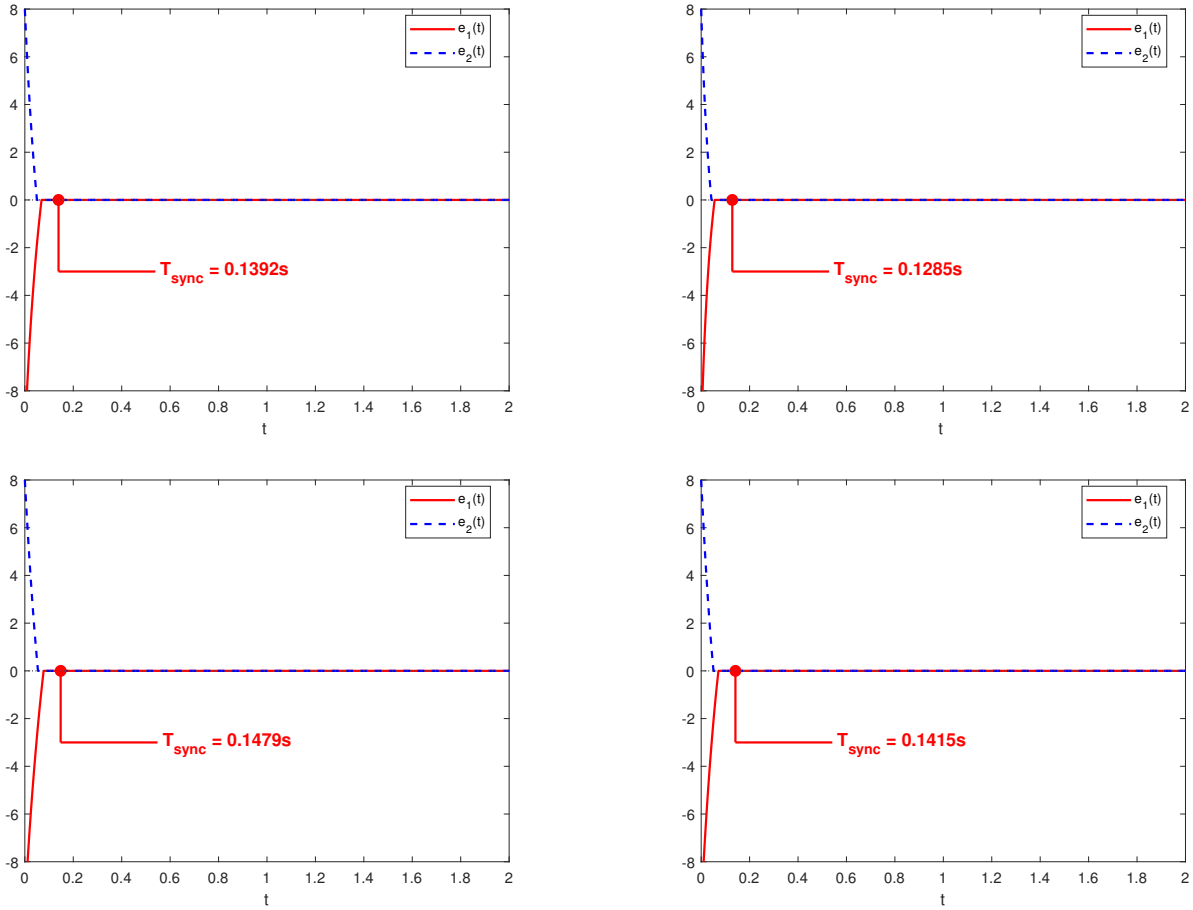

Figure 9. Example 4.7 systematic error curve.

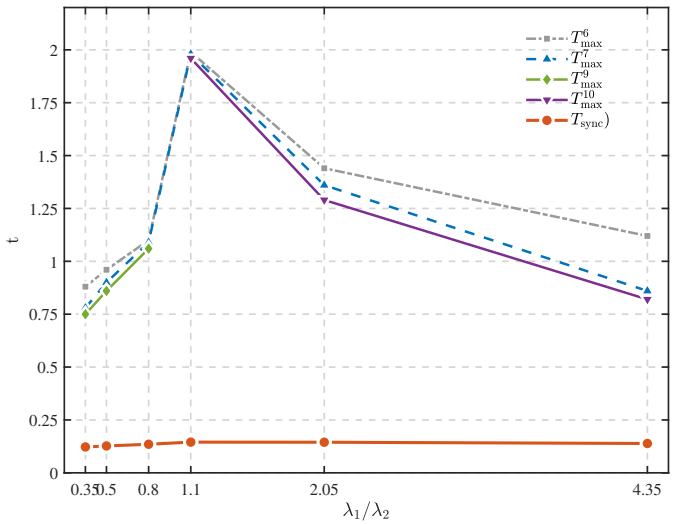

Figure 10. Comparison of theoretical upper bounds and actual synchronization times under different λ_1/λ_2 ratios.

Table 1. Comparison of theoretical and actual synchronization times under different parameter ratios.

$T_{\max}$ \ λ_1/λ_2	0.35	0.80	2.05	4.35
T_{sync}	0.1285	0.1392	0.1479	0.1415
$T^8_{\max}$	0.67	1.00	1.37	0.94
$T^9_{\max}$	0.80	1.25	\	\
$T^{10}_{\max}$	\	\	1.66	1.14

Remark 4.2. *The aforementioned numerical simulations compare the proposed theorem with several other lemmas across four distinct scenarios, all conducted under the condition that θ_1 and θ_2 remain invariant. The analysis of Figure 10 indicates that within the framework of Theorem 3.1, when the exponents are fixed, a larger value of $|\lambda_1 - \lambda_2|$ leads to a shorter synchronization time required by the system. This phenomenon is primarily driven by the synergetic coupling effect of the proposed partitioned integration strategy, which exerts a more adaptive driving force across distinct error sub-intervals, effectively overcoming the estimation conservatism inherent in traditional simple algebraic superposition. Therefore, in practical applications, appropriate values of λ_1 and λ_2 can be selected according to specific design needs to satisfy synchronization requirements.*

Remark 4.3. *In the numerical simulations, the initial values and are selected arbitrarily to verify that the fixed-time synchronization is independent of initial conditions. Furthermore, the controller gain is chosen to strictly satisfy the theoretical threshold defined in (2.7) to ensure the negativity of the Lyapunov derivative. It should be noted that for a fair and rigorous comparison, the exact same set of simulation parameters and initial values is utilized when evaluating Theorems 3.2, 3.3, and 3.5. This variable-control approach ensures that the improvement in the settling time estimate is*

purely attributable to the refined mathematical strategy of Theorem 3.1 rather than specific parameter adjustments.

Remark 4.4. *It should be noted that while the numerical examples presented in this section employ a low-dimensional neural network model to ensure the clarity of visual demonstrations and the intuitive comparison of theoretical time bounds, the proposed synchronization scheme is intrinsically scalable to complex, high-dimensional, and large-scale networks. From a theoretical perspective, the network dimension n is rigorously incorporated into the structural design of the Lyapunov functional* $V(t) = \frac{1}{2}\sum_{i=1}^{n} e_i^2(t)$ *and is explicitly accounted for in the derivation of the global parameter* λ_2 *(e.g.,* $\lambda_2 = 2^{(\theta_2+1)/2} n^{(1-\theta_2)/2} \min\{\xi_{5i}\}$*). Consequently, the mathematical validity of Theorem 3.1 and the corresponding control strategies remain robust regardless of the scale of the memristive neural networks, demonstrating broad universality for high-dimensional practical implementations.*

5. Conclusions

This paper has investigated the fixed-time synchronization problem for a class of MNNs with time-varying delays. The primary contribution of this work is the proposal of an improved settling time estimation theorem. Unlike traditional methods that simply superimpose the time bounds of two convergence stages, the proposed theorem employs a partitioned integration analysis based on the magnitude relationship between the control gains λ_1 and λ_2. Both theoretical analysis and numerical comparisons demonstrate that this method significantly reduces the conservatism of the settling time estimation compared to standard lemmas in existing literature. Furthermore, the simulation results delve into the specific relationship between the system convergence rate and the difference $|\lambda_1 - \lambda_2|$, revealing a positive correlation when the exponential parameters are fixed. However, it is important to recognize that while the segmented integration strategy presented in this work provides high-precision estimation, its implementation relies on a five-term controller structure, which entails a higher degree of complexity compared to conventional designs. This complexity potentially increases hardware resource consumption and computational overhead in memristive circuit implementations.

In future research, these theoretical results will be extended to more complex dynamical networks, such as fractional-order MNNs or systems subject to stochastic perturbations. Additionally, designing a dynamic event-triggering mechanism or developing a more efficient controller based on the theory presented in this paper to optimize control energy consumption while maintaining the property of timely convergence is a topic worthy of further exploration.

Author contributions

Junfeng Tong and Minghui Jiang contributed to the study conception and design. All authors contributed to data analysis and manuscript preparation. All authors read and approved the final manuscript.

Use of Generative-AI tools declaration

The authors declare they have not used Artificial Intelligence (AI) tools in the creation of this article.

Acknowledgments

We sincerely appreciate all contributors for their valuable insights and constructive suggestions.

Conflict of interest

All authors declare no conflicts of interest in this paper.

References

1. S. Haykin, *Neural networks and learning machines*, 3 Eds., Pearson, Upper Saddle River, 2009.
2. C. M. Bishop, *Pattern recognition and machine learning*, Springer, New York, 2006.
3. J. J. Hopfield, Neural networks and physical systems with emergent collective computational abilities, *Proc. Natl. Acad. Sci. USA*, **79** (1982), 2554–2558. https://doi.org/10.1073/pnas.79.8.2554
4. D. B. Strukov, G. S. Snider, D. R. Stewart, R. S. Williams, The missing memristor found, *Nature*, **453** (2008), 80–83. https://doi.org/10.1038/nature06932
5. L. Chua, Memristor—the missing circuit element, *IEEE T. Circ. Theor.*, **18** (1971), 507–519. https://doi.org/10.1109/TCT.1971.1083337
6. A. Wu, Z. Zeng, Exponential stabilization of memristive neural networks with time delays, *IEEE T. Neural Net. Lear.,* **23** (2012), 1919–1929.
7. Z. Wang, J. Cao, G. Lu, J. H. Park, Fixed-time passification analysis of interconnected memristive reaction-diffusion neural networks, *IEEE T. Netw. Sci. Eng.*, **7** (2020), 1814–1824. https://doi.org/10.1109/TNSE.2019.2953846
8. M. Chen, X. Luo, Y. Zhang, H. Wu, Q. Xu, B. Bao, Initial-boosted behaviors and synchronization of memristor-coupled memristive systems, *IEEE T. Circuits-I*, **70** (2023), 5433–5445. https://doi.org/10.1109/TCSI.2023.3326341
9. L. Hua, H. Zhu, K. Shi, S. Zhong, Y. Tang, Y. Liu, Novel finite-time reliable control design for memristor-based inertial neural networks with mixed time-varying delays, *IEEE T. Circuits-I*, **68** (2021), 1599–1609. https://doi.org/10.1109/TCSI.2021.3052210
10. Z. Han, N. Chen, X. Wei, M. Yuan, H. Li, Projective synchronization of delayed uncertain coupled memristive neural networks and their application, *Entropy,* **25** (2023), 1241. https://doi.org/10.3390/e25081241
11. Y. Cao, C. Cai, X. Xu, X. Bi, Cross-channel color image encryption scheme based on discrete memristive coupled neurons and DWT compression, *Electronics*, **13** (2024), 2647. https://doi.org/10.3390/electronics13132647
12. P. J. Uhlhaas, W. Singer, Neural synchrony in cortical networks: Mechanisms and implications for neural information processing and coding, *Neuron*, **52** (2006), 155–168. https://doi.org/10.1016/j.neuron.2006.09.020
13. S. Chen, J. Cao, Projective synchronization of neural networks with mixed time-varying delays and parameter mismatch, *Nonlinear Dyn.*, **67** (2012), 1397–1406.

14. L. Chen, J. Lu, Cluster synchronization in a complex dynamical network with two nonidentical clusters, *J. Syst. Sci. Complex*, **21** (2008), 20–33.

15. J. Cao, J. Wang, Global asymptotic stability of a general class of recurrent neural networks with time-varying delays, *IEEE Trans. Circuits Syst. I, Fundam. Theory Appl.*, **50** (2003), 34–44. https://doi.org/10.1109/TCSI.2002.807494

16. R. Brayton, C. Tong, Constructive stability and asymptotic stability of dynamical systems, *IEEE T. Circuits Syst.*, **27** (1980), 1121–1130. https://doi.org/10.1109/TCS.1980.1084749

17. F. Huang, Strong asymptotic stability of linear dynamical systems in Banach spaces, *J. Differ. Equ.*, **104** (1993), 307–324. https://doi.org/10.1006/jdeq.1993.1074

18. B. Zhou, On asymptotic stability of linear time-varying systems, *Automatica*, **68** (2016), 266–276. https://doi.org/10.1016/j.automatica.2015.12.030

19. F. Amato, R. Ambrosino, M. Ariola, C. Cosentino, G. De Tommasi, *Finite-time stability and control*, Lecture Notes in Control and Information Sciences, Springer, **453** (2014).

20. S. P. Bhat, D. S. Bernstein, Finite-time stability of continuous autonomous systems, *SIAM J. Control Optim.*, **38** (2000), 751–766. https://doi.org/10.1137/S0363012997321358

21. Y. Hong, J. Huang, Y. Xu, On an output feedback finite-time stabilization problem, *IEEE Trans. Autom. Control*, **53** (2008), 1702–1707. https://doi.org/10.1109/9.905699

22. X. Yang, D. W. C. Ho, Synchronization of delayed memristive neural networks: Robust analysis approach, *IEEE Trans. Cybern.*, **46** (2016), 3377–3387. https://doi.org/10.1109/TCYB.2015.2505903

23. A. Polyakov, Nonlinear feedback design for fixed-time stabilization of linear control systems, *IEEE Trans. Autom. Control*, **57** (2012), 2106–2110. https://doi.org/10.1109/TAC.2011.2179869

24. Y. Xu, X. Wu, C. Xu, Synchronization of time-varying delayed neural networks by fixed-time control, *IEEE Access*, **6** (2018), 2169–3536. https://doi.org/10.1109/ACCESS.2018.2883417

25. C. Chen, L. Li, H. Peng, Y. Yang, L. Mi, H. Zhao, A new fixed-time stability theorem and its application to the fixed-time synchronization of neural networks, *Neural Netw.*, **123** (2020), 412–419. https://doi.org/10.1016/j.neunet.2019.12.028

26. J. Cao, R. Li, Fixed-time synchronization of delayed memristor-based recurrent neural networks, *Sci. China Inf. Sci.*, **60** (2017), 032201. https://doi.org/10.1007/s11432-016-0555-2

27. N. Li, X. Wu, J. Feng, Y. Xu, J. Lü, Fixed-time synchronization of coupled neural networks with discontinuous activation and mismatched parameters, *IEEE T. Neur. Net. Lear.*, **32** (2021), 2470–2482. https://doi.org/10.1109/TNNLS.2020.3005945

28. S. Gong, Z. Guo, S. Wen, T. Huang, Finite-time and fixed-time synchronization of coupled memristive neural networks with time delay, *IEEE Trans. Cybern.*, **51** (2021), 2944–2955. https://doi.org/10.1109/TCYB.2019.2953236

29. W. Yang, Y. W. Wang, I. C. Morărescu, X. K. Liu, Y. Huang, Fixed-time synchronization of competitive neural networks with multiple time scales, *IEEE T. Neur. Net. Lear.*, **33** (2022), 4133–4138. https://doi.org/10.1109/TNNLS.2021.3052868

30. J. P. Aubin, H. Frankowska, *Differential inclusions: Set-valued analysis*, Modern Birkhäuser Classics, Springer, Boston, 2009. https://doi.org/10.1007/978-0-8176-4848-0

31. G. V. Smirnov, *Introduction to the theory of differential inclusions*, Graduate Studies in Mathematics, American Mathematical Society, **41** (2002).

32. G. Hardy, J. Littlewood, G. Polya, *Inequalities*, Cambridge University Press, 1952.

33. S. E. Parsegov, A. E. Polyakov, P. S. Shcherbakov, Nonlinear fixed-time control protocol for uniform allocation of agents on a segment, *Dokl. Math*, **87** (2013), 133–136. https://doi.org/10.1134/S106456241301033X

AIMS Press

© 2026 the Author(s), licensee AIMS Press. This is an open access article distributed under the terms of the Creative Commons Attribution License (https://creativecommons.org/licenses/by/4.0)